Newly Synthesized Proteins

Deutsche Ausgabe: DOI: 10.1002/ange.201511030
Internationale Ausgabe: DOI: 10.1002/anie.201511030

Puromycin Analogues Capable of Multiplexed Imaging and Profiling of Protein Synthesis and Dynamics in Live Cells and Neurons

*Jingyan Ge, Cheng-Wu Zhang, Xue Wen Ng, Bo Peng, Sijun Pan, Shubo Du, Danyang Wang, Lin Li, Kah-Leong Lim, Thorsten Wohland, and Shao Q. Yao**

Abstract: *Newly synthesized proteins constitute an important subset of the proteome involved in every cellular process, yet existing chemical tools used to study them have major shortcomings. Herein we report a suite of cell-permeable puromycin analogues capable of being metabolically incorporated into newly synthesized proteins in different mammalian cells, including neuronal cells. Subsequent labeling with suitable bioorthogonal reporters, in both fixed and live cells, enabled direct imaging and enrichment of these proteins. By taking advantage of the mutually orthogonal reactivity of these analogues, we showed multiplexed labeling of different protein populations, as well as quantitative measurements of protein dynamics by fluorescence correlation spectroscopy, could be achieved in live-cell environments.*

Protein synthesis and degradation underlie a variety of biological processes that manage the organization and function of cells. Dynamic modulation in cellular protein activity and trafficking further manifest cellular response to environment changes during cell proliferation and differentiation.[1] For example, the development of many diseases are caused by abnormal levels of protein expression and activation.[2] Protein synthesis in neurons is implicated in synaptic plasticity and memory processing.[3] Studies of newly synthesized proteins enable direct correlation of protein expression with mRNA expression levels and allow differentiation of primary protein synthesis caused by external stimuli. Our recent interest in the study of newly synthesized proteins and their post-translational modifications (PTMs) has prompted us to ask the next important question: is it possible to visualize, with sufficient spatiotemporal resolutions, newly synthesized proteins and quantify their dynamics in living cells and neurons?[4] Such questions are essential to reveal potential roles that these proteins play in human diseases including neurological disorders.

Traditionally, newly synthesized proteins are monitored by labeling of cells with radioactive amino acids. More recently, metabolic labeling with methionine (Met) surrogates such as azidohomoalanine (AHA) and homopropargylglycine (HPG), coupled with Cu^{I}-catalyzed azide–alkyne cycloaddition (CuAAC), has been developed.[5] By combining with fluorescence imaging and/or mass spectrometric techniques, this BONCAT (bioorthogonal noncanonical amino acid tagging) technique has been used in mammalian cell cultures to analyze changes of newly synthesized proteins.[6] Despite its operational simplicity, this method has major drawbacks. First, metabolic incorporation needs to be performed in Met-free media due to preferential recognition of Met over AHA/HPG by the native cellular machinery. Second, the need for AHA/HPG to be converted into aminoacyl-tRNAs prior to protein synthesis limits its temporal resolution. Finally, both AHA and HPG are incorporated throughout the entire polypeptide chain to generate full-length proteins. Further compounding these shortcomings is the incompatibility of the method with live-cell imaging, due to use of terminal alkyne-containing HPG which needs cytotoxic Cu^{I} catalysts in CuAAC, although in a recent example, copper-free click chemistry was used to successfully image AHA-labeled proteins located on the membrane of live hippocampal neurons.[6b]

In another approach, the antibiotic puromycin (Figure 1 A; labeled as **PO**) is used to label and image newly synthesized proteins.[7,8] As a tyrosyl-tRNA mimic, **PO** binds to the ribosome A-site, is incorporated into the elongating polypeptides, and subsequently causes inhibition of protein synthesis (Supporting Information, Figure S1). When used in minimal amounts, it is exclusively attached to the *C*-terminal end of newly synthesized proteins, thus releasing **PO**-labeled proteins (both truncated and full-length). This so-called "puromycylation" reaction has been studied by western blotting (WB), immunofluorescence (IF), flow cytometry, and mass spectrometry (MS) with **PO**-specific antibodies.[7] Owing to inaccessibility of antibodies through the cell membrane, it is only suitable for fixed cells. During our effort to develop chemical tools capable of imaging newly synthesized proteins in live cells and neurons, we came across

[*] Dr. J. Ge, X. W. Ng, B. Peng, S. Pan, S. Du, D. Wang, Prof. Dr. T. Wohland, Prof. Dr. S. Q. Yao
Department of Chemistry
National University of Singapore
3 Science Drive 3, Singapore 117543 (Singapore)
E-mail: chmyaosq@nus.edu.sg
Dr. J. Ge
Institute of Bioengineering
Zhejiang University of Technology
Hangzhou (China)
Dr. C.-W. Zhang, Prof. Dr. L. Li
Key Laboratory of Flexible Electronics &
Institute of Advanced Materials, Nanjing Tech University
Nanjing, 211816 (China)
Dr. C.-W. Zhang, Dr. K.-L. Lim
National Neuroscience Institute
Singapore 308433 (Singapore)
Prof. Dr. T. Wohland
Department of Biological Sciences
National University of Singapore (Singapore)

Supporting information for this article can be found under: http://dx.doi.org/10.1002/anie.201511030.

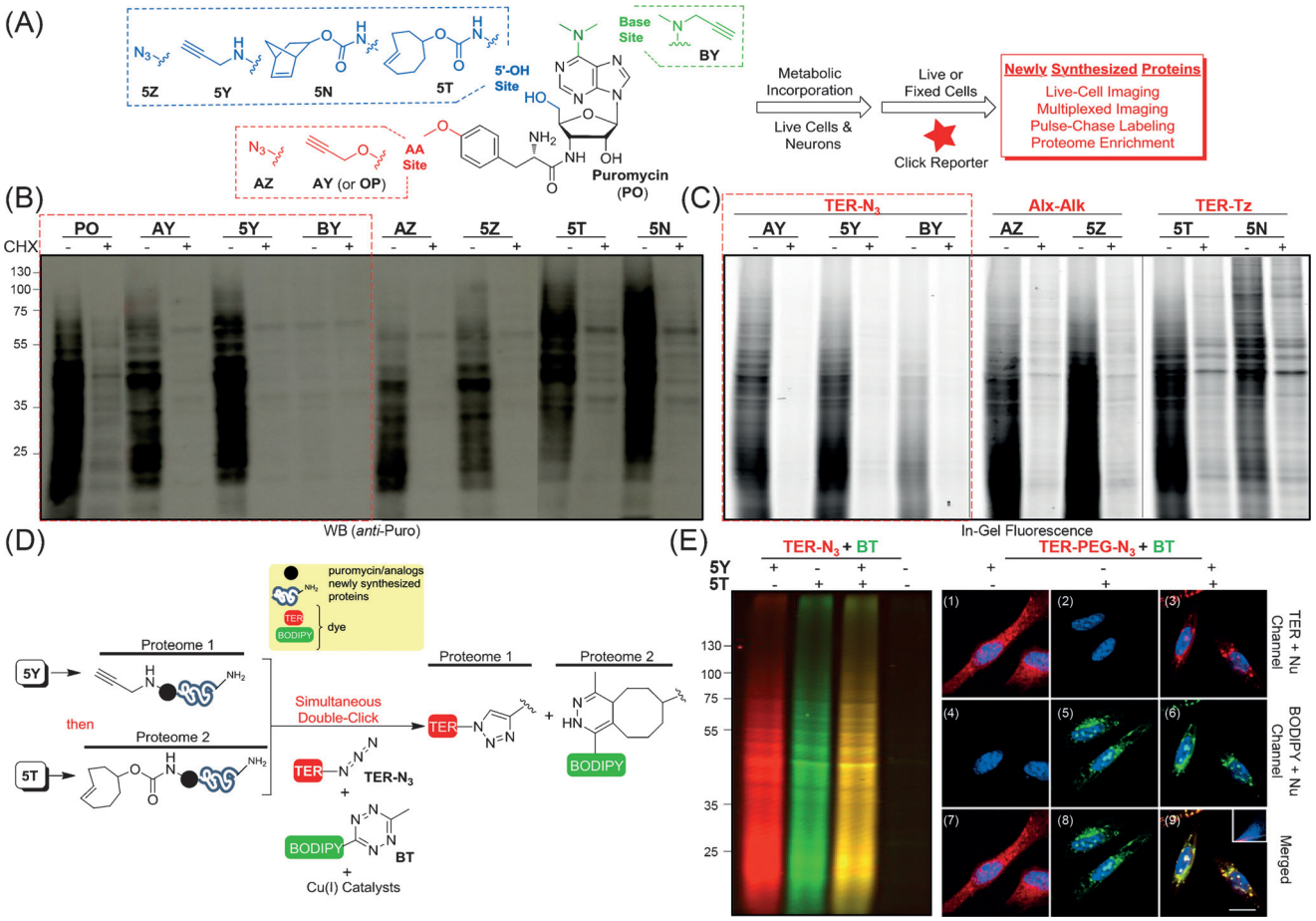

Figure 1. A) Structures of puromycin (**PO**) and various **PO** analogues, including the previously reported **AY**, and newly developed analogues with structural changes at AA-site (red), 5′-OH site (blue), and base site (green). For full structures of analogues and corresponding click reporters, see the Supporting Information, Table S1. B) Puromycin incorporation (10 μM for 4 h) to newly synthesized proteins, with or without CHX pre-treatment (0 or 50 μg mL^{-1} for 1 h) in HeLa cells as determined by WB with anti-puromycin antibody. As the sensitivity of anti-puromycin antibody against puromycin analogues differed, WB gels had to be exposed individually. The loading controls (anti-GAPDH) are shown in the Supporting Information, Figure S4A. C) In-gel fluorescence scanning of newly synthesized proteins from HeLa cells incorporated with puromycin analogues (10 μM for 4 h), followed by cell fixation and click chemistry with the indicated reporter. Upon cell lysis, the lysates were separated on SDS-PAGE and scanned at the fluorophore channel. The coomassie loading controls are shown in the Supporting Information, Figure S4C. D) Sequential labeling of newly synthesized proteins in HeLa cells with **5Y** and **5T** (10 μM each for 4 h), followed by cell fixation and simultaneous double-click labeling with an 1:1 mixture of **TER-N$_3$** and **BT** (1 μM for 1 h). E) In-gel fluorescence scanning profiles of the corresponding cell lysates (left) and imaging results of fixed cells (right) as shown in (D). Red/green: click reporter channel; blue: Hoechst nuclear stain. Panels 7–9: merged images of panels 1/4, 2/5 and 3/6. Inset: colocalization analysis of panel 3/6 (giving $R = 0.89$). Scale bar: 15 μm. See the Supporting Information, Figure S9 for loading controls.

a novel method developed by Salic et al. in which a terminal alkyne-containing **PO** analogue, O-propargyl-puromycin (**OP** in Figure 1 A, renamed as **AY** henceforth), was effective in puromycylation reaction and used to image newly synthesized proteins by combining with CuAAC.[8] Although the method itself was not compatible with live-cell imaging because of the terminal alkyne handle in **AY**, we reasoned that it may be improved by introducing other biocompatible tags that do not need Cu^{I} or other cytotoxic reagents.[9] We also hoped to develop new **PO**-based pairs that could be used in multiplexed experiments similar to the AHA/HPG pair.[10] **PO** is known to be reasonably amenable to structural modifications,[11] and several **PO**-modified probes were already used in cell-free protein synthesis systems (Supporting Information, Figure S1B);[12] in some cases, significant changes at the 5′-OH site of the aminonucleoside structure were tolerated. Herein, we report the development of six new **PO** analogues (**AZ**/**BY**/**5N**/**5T**/**5Y**/**5Z** in Figure 1 A), all of which were capable of puromycylation in live mammalian cells, albeit with different incorporation efficiencies, and could be used for subsequent imaging and profiling of newly synthesized proteins. By taking advantage of the mutual orthogonality in some probes (**5Y**/**5T** and **5Z**/**5T**), we showed they could be used in multiplexed experiments for labeling and simultaneous imaging of different protein populations, under both fixed and live-cell conditions. Protein enrichment and identification were confirmed with select probes by large-scale pull-down (PD)/LC-MS/MS experiments. Finally, quantita-

tive measurement of protein dynamics was performed with labeled live mammalian cells and neurons by fluorescence correlation spectroscopy (FCS).

We first designed and synthesized two new **PO** analogues, **5Y** and **BY** (Supporting Information, Scheme S1). Together with the reported **AY**, each analogue has a terminal alkyne substituted at the AA, 5′-OH and the base site, respectively (Figure 1 A). The puromycylation reaction of newly synthesized proteins from HeLa cells, followed by SDS-PAGE/WB analysis with anti-puromycin antibody (Figure 1 B), and in-gel fluorescence scanning of the corresponding fluorescently labeled protein lysates (with respective click reporters; Figure 1 C), indicate successful metabolic incorporation of all three analogues in a concentration-dependent manner (Supporting Information, Figure S2), although the rate of **BY** incorporation was significantly lower than that of **PO**, **AY** or **5Y** (boxed in red; Figure 1 B,C). Large-scale PD/LC-MS/MS experiments showed similar trends, resulting in positive identification of newly synthesized proteins from various subcellular compartments (Supporting Information, Figure S3). Pretreatment of cells with cycloheximide (CHX, a protein synthesis inhibitor[13]) nearly abolished the incorporation (Figures 1 B,C; Supporting Information, Figure S4). With these findings, and in consideration of synthetic accessibility, the 5′-OH of **PO** was thus chosen as the preferred site for most of our subsequent modifications; we made **5Z**/**5N**/**5T**, having $-N_3$, norbornene, and *trans*-cyclooctene (TCO), respectively, located at the 5′-OH site, as well as **AZ** which has $-N_3$ at the AA site (further structural changes at AA site were not tolerated; data not shown). Similar metabolic incorporation experiments indicate all new analogues (except **BY**) were nearly as effective as **AY** and **5Y** (Figures 1 B,C; Supporting Information, Figure S2), a conclusion also supported by the corresponding IF experiments (Supporting Information, Figure S5). By taking advantage of the clickable tag in each **PO** analogue, direct in-cell imaging of **PO**-labeled newly synthesized proteins was carried out by treatment of fixed cells with suitable fluorescent reporters (Supporting Information, Figure S6); most labeled cells except those from **BY**-incorporated experiments showed varying degrees of fluorescence signals distributed throughout the cytosol and nucleus, while DMSO-treated control cells showed minimal background fluorescence. This indicates our newly developed **PO** analogues were indeed suitable for labeling and imaging of newly synthesized proteins from mammalian cells. Representative analogues were further shown to work well in other mammalian cells and primary neurons (Supporting Information, Figures S7). By striking a balance between labeling newly synthesized proteins with these new puromycin analogues, and their cytotoxicity at higher concentrations (as protein synthesis inhibitors; Supporting Information, Figures S2 and S8), we found most probes worked well at 10 μM, thus this concentration was chosen for subsequent experiments.

Encouraged by above results, we next investigated whether these new **PO** analogues could be used in pulse–chase experiments for multiplexed labeling of two temporally defined sets of newly synthesized proteins (Figure 1 D,E). The AHA/HPG pair was previously used in similar experiments.[10] Mindful of the potential photolability of **AZ** owing to its photoreactive aryl azide moiety,[14] we chose **5Y**/**5T** over **5Y**/**5Z** (a natural surrogate pair of HPG/AHA), because it enabled simultaneous double-click labeling with an 1:1 mixture of **TER-N$_3$** and **BT** reporters in the presence of Cu^I catalysts (Figure 1 D). Possible cross-reactivity between azide/TCO was previously shown to be low.[15] As proof-of-concept experiments, we chose 4 h incorporation windows to achieve maximum protein labeling signals, although a shorter incubation time may be suitable as well (Supporting Information, Figure S9). As shown in Figure 1 E, sequential incubation of live HeLa cells with **5Y** and **5T**, followed by (**TER-N$_3$** + **BT**) treatment, produced two populations of labeled proteins as shown in both the in-gel fluorescence profiles (left) and imaging results (right). Cross-background labeling was not detected in cells treated with **5Y** or **5T** alone (panels 1/2/4/5/7/8). By monitoring elF2α phosphorylation (a cell stress marker[8a]), we detected no apparent cellular stress under our labeling conditions due to formation of truncated proteins (Supporting Information, Figure S9). While **5Y**-treated cells showed a diffuse labeling pattern (panel 1), a small number of punctate stains were observed in **5T**-labeled cells (panel 5). Furthermore, the cellular distribution of their fluorescence signals appeared to be slightly different. This was despite the fact that in our earlier IF experiments (Supporting Information, Figure S5), most analogues showed similar staining patterns. We therefore evaluated whether different puromycin analogues, possibly due to the minor difference in their ribosome A-site affinity as a result of structural variation, might cause the newly synthesized proteins to degrade or aggregate differently (Supporting Information, Figure S10); while protein degradation rates for most analogues were similar, the molecular weight distribution, as well as the relative amounts of soluble/insoluble proteins, varied slightly. We thus concluded that **5Y**/**5T** pair is indeed suitable for pulse-chase multiplexed labeling experiments.

We next assessed whether the imaging experiments could be performed in live cells, by using the **5Z**/**5T** pair (Figure 2), which may be click-labeled by reporters containing dibenzylcyclooctyne (DBCO) and tetrazine, respectively, under copper-free conditions.[9] We first optimized the types of fluorophores suitable for live-cell imaging experiments (Supporting Information, Figures S11–13 and Movie S1); both **FITC-DBCO** and **TMR-DBCO** were suitable for imaging **5Z**-labeled, newly synthesized proteins. For **5T**-labeled proteins, **FITC-Tz** and **TMR-Tz** were suitable reporters. Interestingly, the two previously reported tetrazine-containing fluorophores,[16] **BT** and **CT**, were found to be mostly trapped in the *endo*/lysosomes under our conditions and not suitable for live-cell imaging. We further confirmed the positive imaging signals were from newly synthesized proteins by blocking protein synthesis with CHX and preventing protein degradation with bortezomib (a proteasome inhibitor; Supporting Information, Figure S11). Finally, we chose **5Z**/**5T** and **TMR-DBCO**/**FITC-Tz** for subsequent multiplexed imaging experiments in live mammalian cells and neurons.

As shown in Figure 2 (see also the Supporting Information, Figure S14), sequential labeling of live HeLa cells with

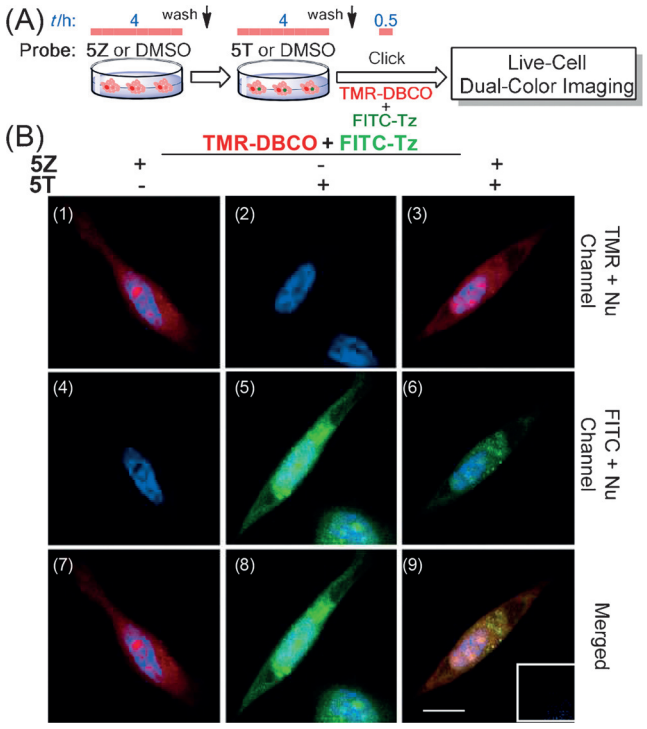

Figure 2. Pulse-chase, multiplexed incorporation, and labeling of newly synthesized proteins in live HeLa cells. A) Sequential treatment of cells with **5Z** and **5T** (10 μM for 4 h each). Live cells were directly stained with an 1:1 click cocktail of **TMR-DBCO**/**FITC-Tz** (1 μM each), and imaged. B) Confocal images of cells from (A), with results from singly treated control cells shown in panels 1/2/4/5/7/8. Inset: colocalization analysis of panel 3/6 (giving $R = 0.87$). Scale bar: 20 μm.

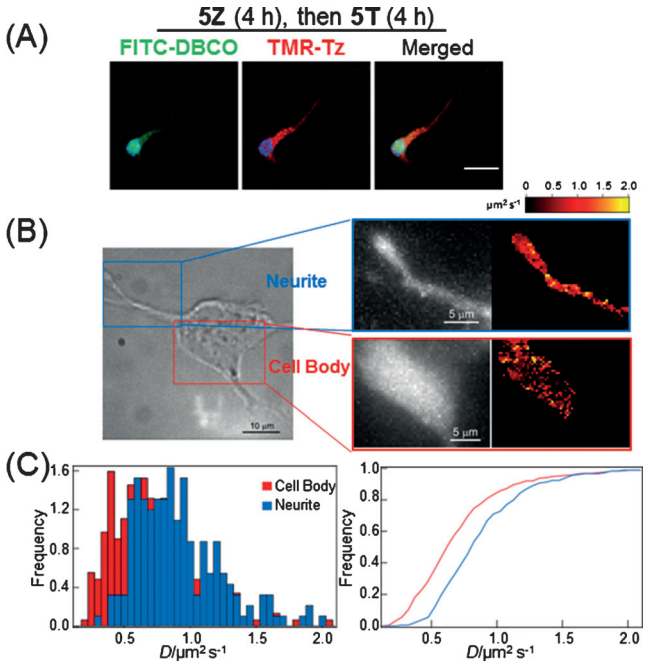

Figure 3. A) Images of live primary neurons sequentially labeled by **5Z**/**5T** (10 μM for 4 h each), followed by direct staining with (**FITC-DBCO** + **TMR-Tz**). Scale bar = 15 μm. B) Wide-field image of a differentiated SH-SY5Y cell (left) indicating the measured regions of neurite (boxed in blue) and cell body (boxed in red). Right: Maps of fluorescence intensity with SPIM illumination and *D*. C) *D* histograms of the neurite and cell body of the SH-SY5Y cell obtained from their respective *D* images (left), and the corresponding cumulative frequency plots of *D* (right).

5Z and **5T** followed by staining of the resulting cells directly with an 1:1 mixture of (**TMR-DBCO** + **FITC-Tz**) led to exclusive labeling of two distinct populations of newly synthesized proteins (panels 3/6/9 in Figure 2B), with no detectable cross-background reactivity in singly labeled cells (panels 1/4/7 & 2/5/8 for **5Z**- and **5T**-labeled cells, respectively). We further confirmed the live-cell imaging capability of **5Z**/**5T** and their corresponding click reporters by successfully carrying out metabolic incorporation and multiplexed imaging experiments in primary neurons (Supporting Information, Figures S15 and Movie S2). The *Z*-scan of stained neurons showed strong fluorescence signals in both the cytosol and nucleus, with occasional punctate stains. These results are similar to those obtained from fixed HeLa cells (Supporting Information, Figure S6), and consistent with previous reports using HPG/AHA incorporation and stimulated Raman scattering imaging with deuterated amino acids.[6b,17]

The clear advantage of our newly developed **PO** analogues lies in their live-cell compatibility, thus enabling imaging of newly synthesized proteins and measurement of their diffusion properties, especially in neurons and neuron-like dendritic cells (Figure 3). Intracellular trafficking of newly synthesized dendritic proteins allows neuronal synapses to respond quickly to stimulation and ensure the plasticity of synaptic connections.[6b] As shown in Figure 3A (see also the Supporting Information, Figure S15), in **5Z**/**5T**-labeled cortex primary neurons stained by (**FITC-DBCO** + **TMR-Tz**), while both FITC and TMR signals were strongly detected in the soma bodies, the consistently stronger and long-lasting TMR signals along the dendrites might be due to faster degradation of **5Z**-labeled proteins, although this was not supported by our data for other cell types (Supporting Information, Figure S10). To analyze the mobility and diffusion dynamics of newly synthesized proteins in differentiated SH-SY5Y cells (a neuronal cell model), we used FCS, which is capable of quantifying the dynamics of fluorescent molecules by analyzing temporal fluctuations of fluorescence signals at single molecule level.[18a] We chose **5Z**/**TMR-DBCO** due to the improved photostability of TMR. Control confocal FCS experiments were first performed on labeled HeLa cells to verify the experimental set-ups (Supporting Information, Figure S16); two diffusive components were detected in the nucleoplasm of cells, attributed to complexes formed from nonspecific TMR labeling ($D = 9.20 \pm 1.77\ \mu m^2 s^{-1}$) and **5Z**-dependent, slower-moving newly synthesized proteins ($D = 0.74 \pm 0.26\ \mu m^2 s^{-1}$), respectively. To investigate the diffusion of the entire population of newly synthesized proteins, we used imaging-based, single-plane illumination microscopy (SPIM)-FCS,[18b] which provides spatial maps of diffusion coefficient (D) and better statistics (Figure 3B,C). The measurements were performed at two different locations of the dendritic cell (neurite and cell body). By focusing on the slow-moving, labeled proteins ($D <$

$2\ \mu m^2 s^{-1}$) in these locations, we found the D distributions were heterogeneous; a difference could be clearly observed between the distributions of D of the cell body ($D = 0.73 \pm 0.40\ \mu m^2 s^{-1}$) and the neurite ($D = 0.90 \pm 0.35\ \mu m^2 s^{-1}$). This difference was readily visible in the cumulative frequency plots shown in Figure 3C. The higher diffusion coefficients of newly synthesized proteins in the neurite might indicate a lower viscosity in the neurite than in the cell body of differentiated SH-SY5Y cells. Our results thus present a non-invasive method to study the dynamics of newly synthesized proteins in live neurons and neuron-like cells.

In conclusion, we have developed a suite of cell-permeable puromycin analogues capable of multiplexed imaging of newly synthesized proteins in live cells and neurons. Diffusion dynamics of newly synthesized proteins inside live neuron-like dendritic cells were quantitatively measured, revealing a heterogeneous behavior. This new method overcame major drawbacks of existing strategies, thus setting the stage to directly image newly synthesized proteins from live tissues and small animals. Further optimization of current live-cell pulse-chase procedures with different puromycin analogues are underway. Additional work is also needed to determine whether these analogues label the same populations of newly synthesized proteins.

Acknowledgements

Funding was provided by the National Medical Research Council (CBRG/0038/2013) and Ministry of Education (MOE2012-T2-2-051 and MOE2013-T2-1-048) of Singapore.

Keywords: bioorthogonality · metabolic incorporation · multiplexed imaging · newly synthesized proteins · puromycin

How to cite: *Angew. Chem. Int. Ed.* **2016**, *55*, 4933–4937
Angew. Chem. **2016**, *128*, 5017–5021

[1] F. U. Hartl, A. Bracher, M. Hayer-Hartl, *Nature* **2011**, *475*, 324–332.
[2] W. E. Balch, R. I. Morimoto, A. Dillin, J. W. Kelly, *Science* **2008**, *319*, 916–919.
[3] M. A. Sutton, E. M. Schuman, *Cell* **2006**, *127*, 49–58.
[4] K. Liu, P.-Y. Yang, Z. Na, S. Q. Yao, *Angew. Chem. Int. Ed.* **2011**, *50*, 6776–6781; *Angew. Chem.* **2011**, *123*, 6908–6913.
[5] J. A. Johnson, Y. Y. Lu, J. A. Van Deventer, D. A. Tirrell, *Curr. Opin. Chem. Biol.* **2010**, *14*, 774–780.
[6] a) D. C. Dieterich, A. J. Link, J. Graumann, D. A. Tirrell, E. M. Schuman, *Proc. Natl. Acad. Sci. USA* **2006**, *103*, 9482–9487; b) D. C. Dieterich, J. J. L. Hodas, G. Gouzer, I. Y. Shadrin, J. T. Ngo, A. Triller, D. A. Tirrell, E. M. Schuman, *Nat. Neurosci.* **2010**, *13*, 897–905; c) K. Eichelbaum, M. Winter, M. B. Diaz, S. Herzig, J. Krijgsveld, *Nat. Biotechnol.* **2012**, *30*, 984–990; d) A. J. M. Howden, V. Geoghegan, K. Katsch, G. Efstathiou, B. Bhushan, O. Boutureira, B. Thomas, D. C. Trudgian, B. M. Kessler, D. C. Dieterich, B. G. Davis, O. Acuto, *Nat. Methods* **2013**, *10*, 343–346.
[7] a) E. K. Schmidt, G. Clavarino, M. Ceppi, P. Pierre, *Nat. Methods* **2009**, *6*, 275–277; b) R. Aviner, T. Geiger, O. Elroy-Stein, *Genes Dev.* **2013**, *27*, 1834–1844; c) F. Buhr, J. Kohl-Landgraf, S. T. Dieck, C. Hanus, D. Chatterjee, A. Hegelein, E. M. Schuman, J. Wachtveitl, H. Schwalbe, *Angew. Chem. Int. Ed.* **2015**, *54*, 3717–3721; *Angew. Chem.* **2015**, *127*, 3788–3792.
[8] a) J. Liu, Y. Xu, D. Stoleru, A. Salic, *Proc. Natl. Acad. Sci. USA* **2012**, *109*, 413–418; b) R. A. J. Signer, J. A. Magee, A. Salic, S. J. Morrison, *Nature* **2014**, *509*, 49–54.
[9] a) E. M. Sletten, C. R. Bertozzi, *Angew. Chem. Int. Ed.* **2009**, *48*, 6974–6998; *Angew. Chem.* **2009**, *121*, 7108–7133; b) R. Selvaraj, J. M. Fox, *Curr. Opin. Chem. Biol.* **2013**, *17*, 753–760.
[10] K. Beatty, D. A. Tirrell, *Bioorg. Med. Chem. Lett.* **2008**, *18*, 5995–5999.
[11] H. Lee, K. L. Fong, R. Vince, *J. Med. Chem.* **1981**, *24*, 304–308.
[12] a) S. R. Starck, X. Qi, B. N. Olsen, R. W. Roberts, *J. Am. Chem. Soc.* **2003**, *125*, 8090–8091; b) Y. Kawahashi, N. Doi, H. Takashima, C. Tsuda, Y. Oishi, R. Oyama, M. Yonezawa, E. Miyamoto-Sato, H. Yanagawa, *Proteomics* **2003**, *3*, 1236–1243; c) L. P. Tan, G. Y. J. Chen, S. Q. Yao, *Bioorg. Med. Chem. Lett.* **2004**, *14*, 5735–5738.
[13] T. Schneider-Poetsch, J. Ju, D. E. Eyler, Y. Dang, S. Bhat, W. C. Merrick, R. Green, B. Shen, J. O. Liu, *Nat. Chem. Biol.* **2010**, *6*, 209–217.
[14] S. Pan, H. Zhang, C. Wang, S. C. L. Yao, S. Q. Yao, *Nat. Prod. Rep.* **2016**, DOI: 10.1039/c5np00101c.
[15] M. R. Karver, R. Weissleder, S. A. Hilderbrand, *Angew. Chem. Int. Ed.* **2012**, *51*, 920–922; *Angew. Chem.* **2012**, *124*, 944–946.
[16] a) L. G. Meimetis, J. C. T. Carlson, R. J. Giedt, R. H. Kohler, R. Weissleder, *Angew. Chem. Int. Ed.* **2014**, *53*, 7531–7534; *Angew. Chem.* **2014**, *126*, 7661–7664; b) J. C. T. Carlson, L. G. Meimetis, S. A. Hilderbrand, R. Weissleder, *Angew. Chem. Int. Ed.* **2013**, *52*, 6917–6920; *Angew. Chem.* **2013**, *125*, 7055–7058.
[17] L. Wei, Y. Yu, Y. Shen, M. C. Wang, W. Min, *Proc. Natl. Acad. Sci. USA* **2013**, *110*, 11226–11231.
[18] a) R. Macháň, T. Wohland, *FEBS Lett.* **2014**, *588*, 3571–3584; b) A. P. Singh, T. Wohland, *Curr. Opin. Chem. Biol.* **2014**, *20*, 29–35.

Received: November 27, 2015
Revised: February 9, 2016
Published online: March 11, 2016

